10

Underground Caves, Tunnels and Excavation of Hydraulic Power Station

10.1 Introduction

Underground caves, excavations or underground openings pose fundamental problems in rock mechanics and geotechnical engineering (Brady and Brown, 1985; Goodman, 1989; Wittke, 1990; Hudson and Harrison, 1997; Sun, 1999; Harrison and Hudson, 2000; Zhou and Yang, 2005). Underground opening includes mines, shafts, tunnels (drifts), hydraulic power plants and chambers for the military, for storage of foods, chemical products, oil and natural gas and for other civil, industrial and war applications. Underground excavation breaks the equilibrium of the original stresses in the rock or soil and causes a redistribution of stress in the surrounding rock or soil. The stress state of an underground circular cave or tunnel is shown in Fig. 10.1. The surrounding rock (or soil) is acted upon under the vertical stress σ_y and the horizontal stress σ_x.

According to the Kirsch formula in rock mechanics, the stresses at the element (point M in Fig. 10.1) within the surrounding rock could be calculated from

$$\sigma_r = \frac{\sigma_x + \sigma_y}{2}(1 - \frac{a^2}{r^2}) - \frac{\sigma_y - \sigma_x}{2}(1 - 4\frac{a^2}{r^2} + 3\frac{a^4}{r^4})\cos 2\theta \tag{10.1a}$$

$$\sigma_\theta = \frac{\sigma_x + \sigma_y}{2}(1 + \frac{a^2}{r^2}) + \frac{\sigma_y - \sigma_x}{2}(1 + 3\frac{a^4}{r^4})\cos 2\theta \tag{10.1b}$$

$$\tau_{r\theta} = \frac{\sigma_y - \sigma_x}{2}(1 + 2\frac{a^2}{r^2} - 3\frac{a^4}{r^4})\sin 2\theta \tag{10.1c}$$

where σ_r, σ_θ and $\tau_{r\theta}(\tau_{r\theta} = \tau_{\theta r})$ are radial, tangential and shear stresses at the

M.-H. Yu et al., *Computational Plasticity*

element, respectively.

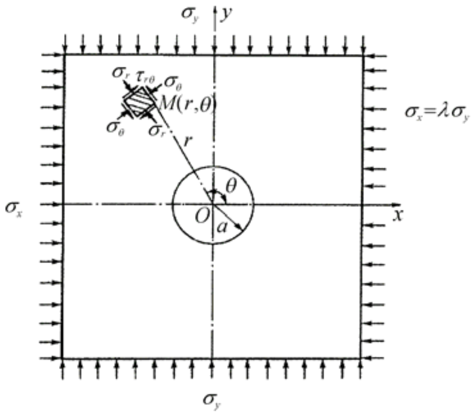

Fig. 10.1 Stress state of an underground circular tunnel

If r is infinite, or R_0=0, the expressions of situ stresses in the polar coordinates system are obtained as follows:

$$\sigma_r = \frac{\sigma_x + \sigma_y}{2} - \frac{\sigma_y - \sigma_x}{2}\cos 2\theta \tag{10.2a}$$

$$\sigma_\theta = \frac{\sigma_x + \sigma_y}{2} + \frac{\sigma_y - \sigma_x}{2}\cos 2\theta \tag{10.2b}$$

$$\tau_{r\theta} = \frac{\sigma_y - \sigma_x}{2}\sin 2\theta \tag{10.2c}$$

The finite element method has now become recognized as a general method of wide applicability to geomechanics and rock engineering. The elasto-plastic FEM or non-linear material problem has also been widely accepted. Descriptions and examples of analysis can be seen in the book of Zienkiewicz (1971). The Mohr-Coulomb criterion, the Drucker-Prager criterion and the no-tension material model were usually used.

Some examples are given to show the effect of the failure criteria on the results. The unified strength theory provides us with a very effective approach for studying the effect of failure criterion on various problems. The plastic analysis of an underground circular excavation (cave or tunnel etc.) is described in this chapter.

Many large hydraulic power plants have been constructed on the Yellow River, Yangtze River and in other regions in China. The stability of the underground cave of a large hydraulic power station has been studied by many researchers. The failure of the surrounding rock mass may be caused by the lower strength of the rock mass somewhere. Also, it may be caused by the accumulation of stress at the underground excavation. The local failure of the rock mass caused by stress accumulation during excavation can be forecast by numerical modeling analysis.

The distribution of the weak positions has a certain regularity, but also has some differences due to the difference in the virginal geo-stress field, the form of excavation, the direction of the excavation's axis, the method of excavating and the choice of yield criterion.

Plastic zones analysis for the stability of the underground cave of a large hydraulic power station based on the twin-shear unified strength theory was carried out during excavation engineering by the Investigation and Design Institute of Northwest China Hydroelectric Power (Liu, 1994; 1995; Liu and Wu, 1995; Sun, 1998). The twin-shear unified strength theory and associated flow rule were implemented in FEM codes and used for several large hydraulic engineering and pumped storage hydraulic power station projects (Sun et al., 2004a; 2004b). The twin-shear unified strength theory is also used for dynamic problems. Dynamic response and blast-resistance analysis of a tunnel subjected to blast loading was conducted successfully by professors Liu and Wang (2004) at Zhejiang University, Hangzhou, China, for a railroad tunnel.

10.2 Effect of Yield Criterion on the Plastic Zone for a Circular Cave

Plastic analysis was calculated for a circular cave under the action of a uniform vertical pressure. The spread of plastic zones in terms of the single-shear theory or the Mohr-Coulomb strength theory and the twin-shear strength theory with material parameter C_0=3 MPa were obtained and shown in Fig. 10.2. The difference between the single-shear theory and the twin-shear theory is obvious.

The plastic zones in terms of the single-shear theory or the Mohr-Coulomb strength theory and the twin-shear strength theory with material parameter C_0=2.6 MPa are given as shown in Fig. 10.3. The difference is also displayed.

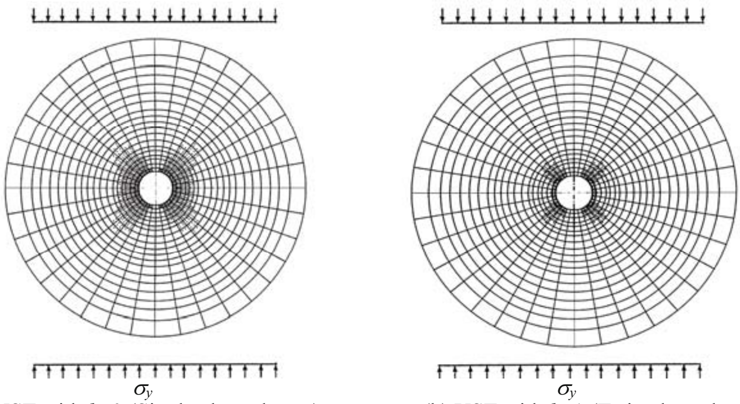

(a) UST with b=0 (Single-shear theory) (b) UST with b=1 (Twin-shear theory)

Fig. 10.2 Distribution of plastic zone around circular cave (C_0= 3.0 MPa)

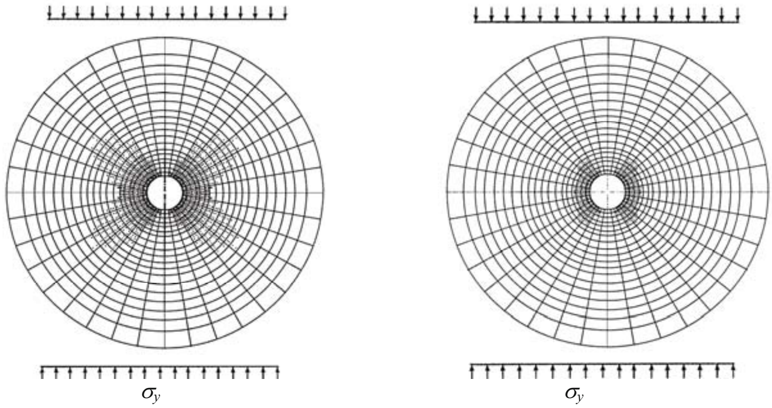

(a) UST with b=0 (Single-shear theory) (b) UST with b=1 (Twin-shear theory)

Fig. 10.3 Distribution of plastic zone around circular cave (C_0= 2.6 MPa)

10.3 Plastic Zone for Underground Circular Cave under Two Direction Compressions

An underground circular cave is under vertical stress and horizontal stress, as shown in Fig. 10.4. The structure is considered a plane strain problem. A series of computational results can be obtained by using the unified strength theory. The ratio of load $\lambda=\sigma_x/\sigma_y$ is referred to as the lateral stress coefficient.

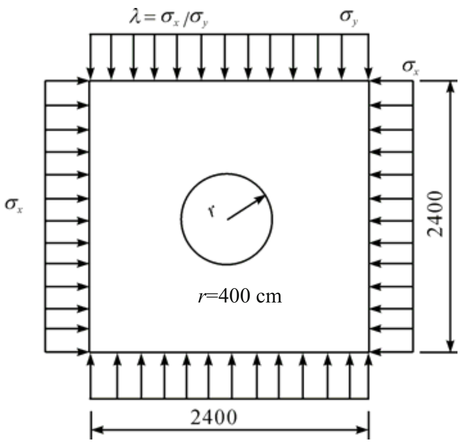

Fig. 10.4 Underground circular cave under vertical stress and horizontal stress

10.3.1 Material Model

Three basic yield criteria of the unified strength theory are chosen for use in geomaterials and geotechnical engineering. They are:

(1) b=0, the single-shear theory, or the Mohr-Coulomb strength theory

$$F = F' = \sigma_1 - \alpha\sigma_3 = \sigma_t \tag{10.3}$$

(2) b=1, the twin-shear strength model (Yu, 1985)

$$F = \sigma_1 - \frac{\alpha}{2}(\sigma_2 + \sigma_3) = \sigma_t, \quad \text{when} \quad \sigma_2 \le \frac{\sigma_1 + \alpha\sigma_3}{1+\alpha} \tag{10.4a}$$

$$F' = \frac{1}{2}(\sigma_1 + \sigma_2) - \alpha\sigma_3 = \sigma_t, \quad \text{when} \quad \sigma_2 \ge \frac{\sigma_1 + \alpha\sigma_3}{1+\alpha} \tag{10.4b}$$

(3) b=1/2, a new yield criterion deduced from the unified strength theory

$$F = \sigma_1 - \frac{\alpha}{3}(\sigma_2 + 2\sigma_3) = \sigma_t, \quad \sigma_2 \le \frac{\sigma_1 + \alpha\sigma_3}{1+\alpha} \tag{10.5a}$$

$$F' = \frac{1}{3}(2\sigma_1 + \sigma_2) - \alpha\sigma_3 = \sigma_t, \quad \sigma_2 \ge \frac{\sigma_1 + \alpha\sigma_3}{1+\alpha} \tag{10.5b}$$

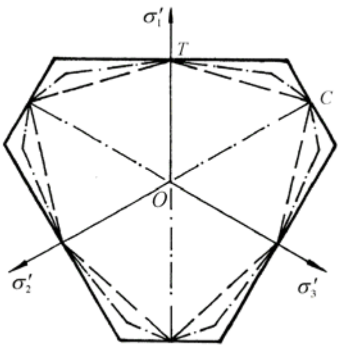

Fig. 10.5 Three fundamental criteria for geomaterials (two bounds and the median)

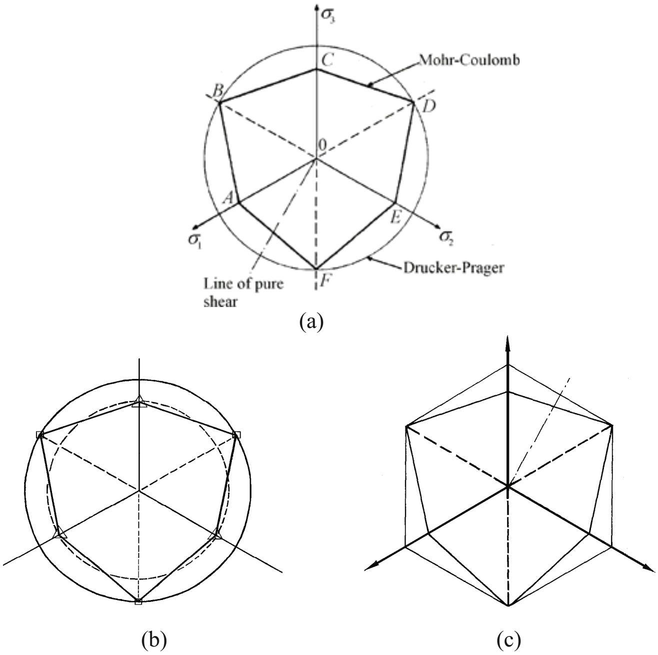

Fig. 10.6 Circle and regular hexagonal cannot match six test points

The Mohr-Coulomb single-shear strength theory, the twin-shear strength theory and this new criterion can be deduced from the unified strength theory when b=0, b=1 and b=1/2, as shown in Fig. 10.5. They are all the piecewise linear yield criteria. The lower bound, upper bound and the median locus situated between these two bounds may be considered as three basic criteria for SD materials.

The circles of the Drucker-Prager criterion cannot match the six experimental points, as shown in Figs. 10.6(a) and 10.6(b). The regular hexagonal also cannot match the six test points, as shown in Fig. 10.6(c).

The new yield criteria given by the unified strength theory with b=1/2 is a median yield criterion between two bounds. It maybe becomes a new reasonable yield criterion instead of the circular cone criteria. The stress angle effect on material strength is not taken into account in various circular cone criteria.

Of course, there is still a need for new models. A general, but simple and thereby well suited model for many potential users may be developed.

10.3.2 Elastic Bearing Capacity

The elastic limits of a structure under six cases of load with $\lambda=\sigma_x/\sigma_y$=1.0, λ=0.75, λ=0.5, λ=0.3, λ=0.2, λ=0 can be obtained by using the unified strength theory.

The elastic limit in terms of the Drucker-Prager criterion is also given for comparison. The results are listed in Table. 10.1.

Table 10.1 Elastic limit of caves under deferent load obtained from deferent criteria

Yield criterion	Elastic limit (MPa)					
	λ=1	λ=0.75	λ=0.5	λ=0.3	λ=0.2	λ=0.0
UST with b=0 (Single-shear theory)	16.31	14.63	13.21	12.25	11.82	11.05
UST with b=0.5	17.51	15,72	14.19	13.16	12.70	11.87
UST with b=1 (Twin-shear theory)	18.19	16.32	14.73	13.67	13.19	12.23
Drucker-Prager criterion	17.42	15.63	14.11	13.09	12.63	11.81

It is shown that the elastic limit of the cave under vertical compression in terms of the unified strength theory with b=1 (i.e. twin-shear theory) is the maximum, and the elastic limit of the unified strength theory with b=0 (i.e. single-shear theory, Mohr-Coulomb strength theory) is the minimum. The results of using unified strength theory with b=1/2 lie between these two limits. It is interesting that the elastic limit of the Drucker-Prager criterion is similar to the elastic limit of the unified strength theory with b=1/2.

10.3.3 Lasto-Plastic Analysis

Choose an 8-node quadrilateral element, mesh the structure into 48 elements with a total of 173 nodes, as shown in Fig. 10.7. A series of computational results using the unified strength theory and unified elasto-plastic constitutive relationship can be obtained. When the load coefficient is $\lambda=\sigma_x/\sigma_y$=0.2, σ_y=20 MPa, by increasing gradually to 30 MPa, then to 34 MPa, the spreads of the plastic zone using the unified strength theory with b=0, b=1/2, and b=1 are shown in Figs. 10.7, 10.8 and 10.9.

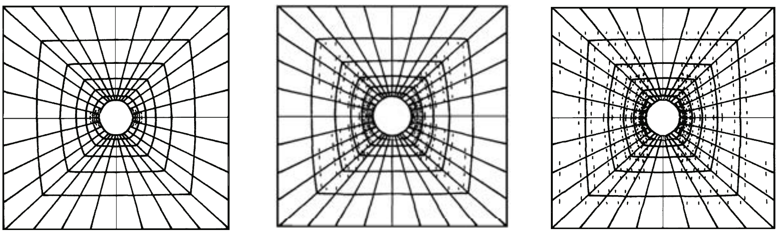

(a) σ_y=20 MPa (b) σ_y=30 MPa (c) σ_y=34 MPa

Fig. 10.7 Spread of plastic zone of a cave using UST with b=0 (Single-shear theory)

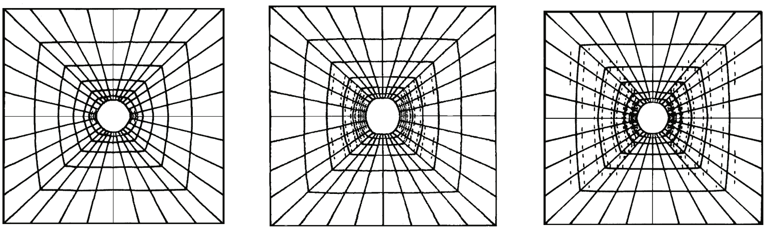

(a) σ_y=20 MPa (b) σ_y=30 MPa (c) σ_y=34 MPa

Fig. 10.8 Spread of plastic zone of a cave using UST with b=1/2 (A new criterion)

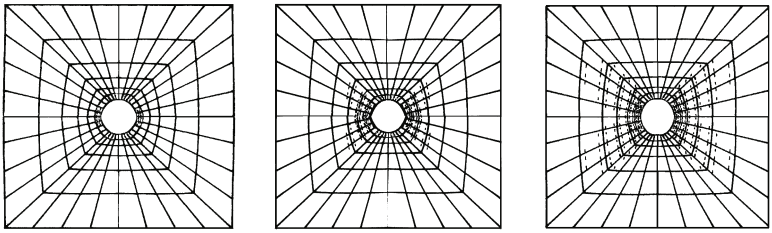

(a) σ_y=20 MPa (b) σ_y=30 MPa (c) σ_y=34 MPa

Fig. 10.9 Spread of plastic zone of a cave using UST with b=1 (Twin-shear theory)

10.3.4 Comparison of Different Criteria

For comparison, three cases of load $\lambda=\sigma_x/\sigma_y=0$, $\lambda=0.2$ and $\lambda=0.5$ are analyzed. The spreads of the plastic zone when σ_y increases gradually from 20 MPa can be obtained. The unified strength theory with b=0, b=1/2 and b=1 and the Drucker-Prager criterion are calculated respectively. The Drucker-Prager criterion is used for comparison

Figures 10.10 and 10.11 are the comparison of the spreads of plastic zones with four criteria when $\lambda=\sigma_x/\sigma_y=0$, i.e. the vertical load only, as σ_y increases from 20 MPa to 24 MPa and 28 MPa.

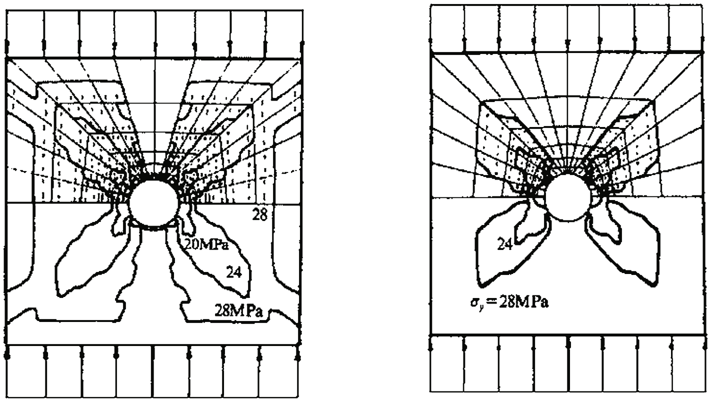

(a) UST with b=0 (Single-shear theory) (b) UST with b=1/2 (New criterion)

Fig. 10.10 Spread of plastic zone of a cave under vertical load (λ=0)

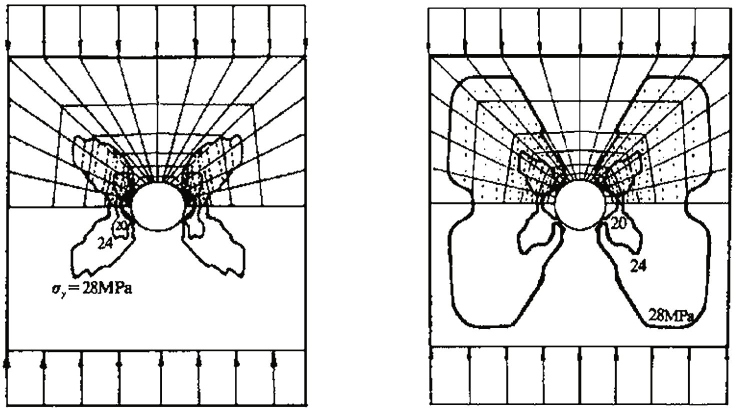

(a) UST with b=1 (Twin-shear theory) (b) Drucker-Prager criterion

Fig. 10.11 Spread of plastic zone of a cave under vertical stress (λ=0)

Figures 10.12 and 10.13 are the comparison of the plastic zones with four criteria when λ=0.2 and σ_y increases from 20MPa to 30 MPa and 34 MPa.

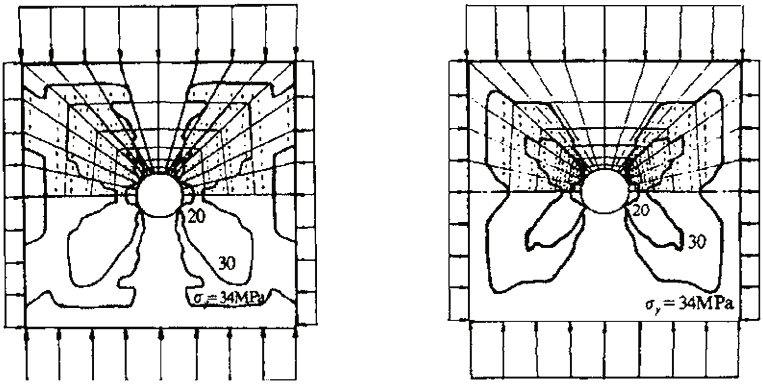

(a) UST with b=0 (Single-shear theory) (b) UST with b=1/2 (New criterion)

Fig. 10.12 Spread of plastic zone of a cave under load λ=0.2

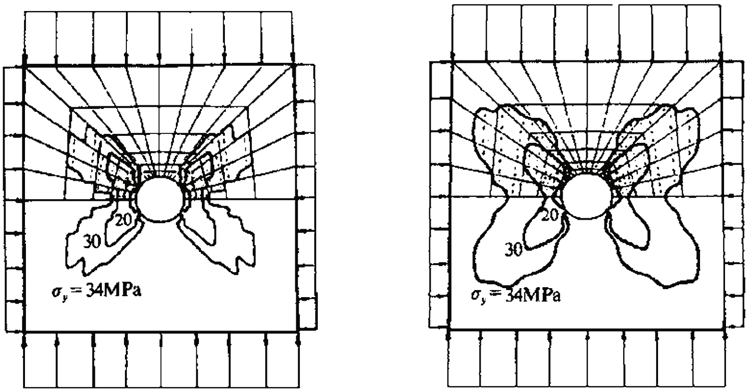

(a) UST with b=1 (Twin-shear theory) (b) Drucker-Prager criterion

Fig. 10.13 Spread of plastic zone of a cave under load λ=0.2

Figures 10.14 and 10.15 are the comparison of the plastic zones with four criteria when $\lambda=\sigma_x/\sigma_y$=0.5 and σ_y increases from 20 MPa to 36 MPa and 44 MPa.

It is seen from the results above that, under the same load, the spread of the plastic zone of an underground cave strongly depends on the choice of the yield criteria, when the unified strength theory parameter b=0, namely single-shear theory (Mohr-Coulomb strength theory), gives the largest plastic zone which has already gone through the periphery of the computational result under σ_y=34 MPa. The unified strength theory with b=1, i.e. the twin-shear strength theory, gives the smallest plastic zone. The unified strength theory with b=0.5 is a new criterion, which gives the median result. These three typical criteria, i.e. two bounds and the median criterion can be adapted for different materials and structures, respectively.

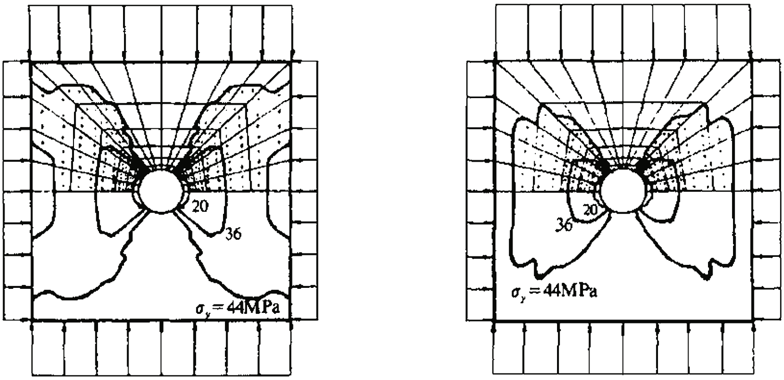

(a) UST with b=0 (Single-shear theory) (b) UST with b=1/2 (New criterion)

Fig. 10.14 Spread of plastic zone of a cave under load λ=0.5

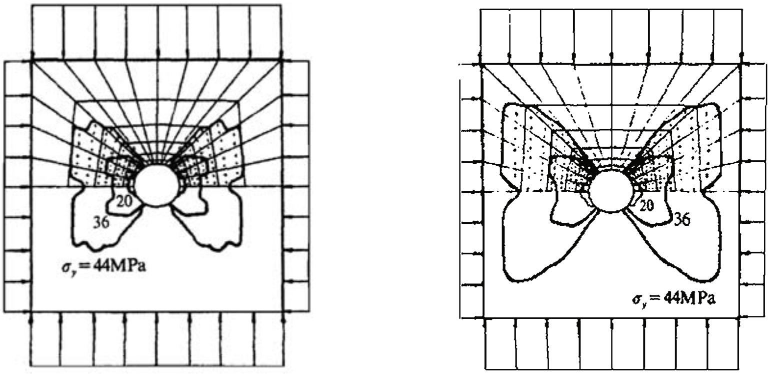

(a) UST with b=1 (Twin-shear theory) (b) Drucker-Prager criterion

Fig. 10.15 Spread of plastic zone of a cave under load λ=0.5

10.4 Laxiwa Hydraulic Power Plant on the Yellow River

The Laxiwa Hydraulic Power Station is the largest power station on the Yellow River. The total installed capacity is 4200 MW, the unit capacity 700 MW, the annual power output 10.223 billion kWh. The power crest elevation is 2460 m, the maximum height 250 m and the total reservoir storage capacity is 1.079 billion cubic meters. Figures 10.16 and 10.17 show pictures of the Laxiwa Hydraulic Power Station and the underground powerhouse cavern. A series of research works were done for the Laxiwa Hydraulic Power Station by Northwest China Hydroelectric Power Investigation and Design Institute. A cross section of the caverns containing the hydroturbine-electric generator and transformer is shown in Fig. 10.18.

Fig. 10.16 Laxiwa Hydraulic Power Station on the Yellow River, China

Fig. 10.17 Large cave of Laxiwa Hydraulic Power Station

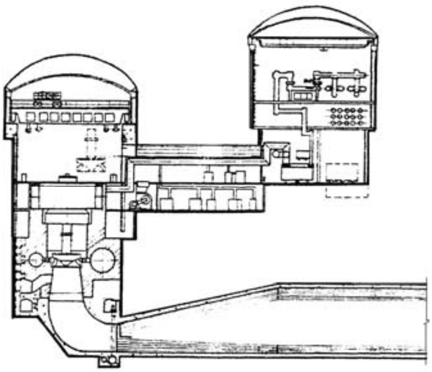

Fig. 10.18 Caverns of hydroturbine electric generator and transformer

Three underground excavations were carried out under the high mountain.

This is a high ground stress area in Laxiwa. The stability of the underground caves is important. So the plastic analysis of the underground excavations were made by An and Hu (1991), Liu and Sun at the Investigation and Design Institute of Northwest China Hydroelectric Power (Liu, 1994; 1995; Liu and Wu, 1995; Sun, 1998; Zhang, 1996). Various yield criteria were used for comparison. The results are given to show the effect of the yield criteria on the analysis. The unified strength theory provides us with a very effective theory and approach for studying the effect of failure criterion on various problems.

The numerical simulation of underground excavation with high ground stress in the area of the Laxiwa Hydraulic Power Plant on the Yellow River, China, was carried out by the Northwest China Hydroelectric Power Investigation and Design Institute (An, 1990; Liu, 1994; 1995; Liu and Hu, 1996; Sun 1998). The dimensions of three underground excavations are shown in Table 10.1.

Table 10.1 Dimensions of three underground excavations

Underground excavation	Maximum (m)	Maximum Height (m)	Height of wall (m)	Total length (m)
1	29	67	50	250
2	23	46	40	224
3	20	57	53	157

The ground stresses can be regarded as a combined stress (σ_x, σ_y, τ_{xy}) acting on the rock around the underground excavation where σ_x=15.3 MPa, σ_y=13.1 MPa, τ_{xy}=0.595 MPa. Figure 10.19 shows the finite element mesh. The plane strain condition is assumed in the FEM analysis. Figures 10.20 and 10.21 show the principal stress trajectory and the maximum principal stress σ_1 and principal stress σ_2 around the caves of the underground excavation under the ground stresses. Displacement of rock around the caves is shown in Fig. 10.22.

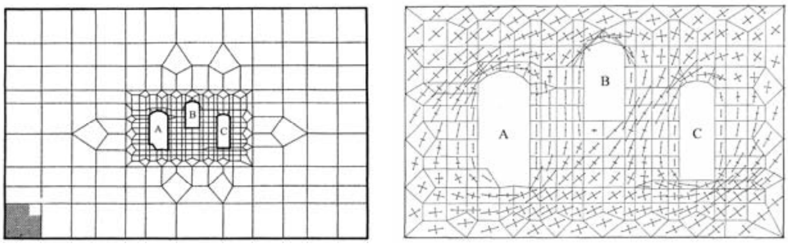

Fig. 10.19 Finite element mesh and principal stress trace around underground excavation

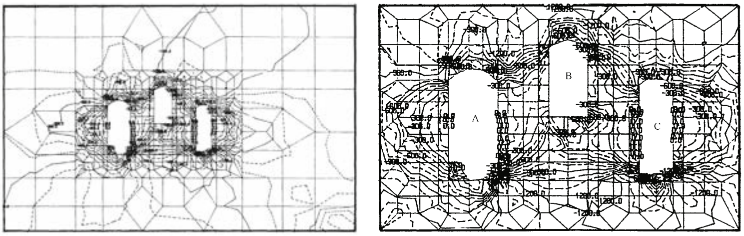

Fig. 10.20 The maximum principal stress σ_1 around the curves

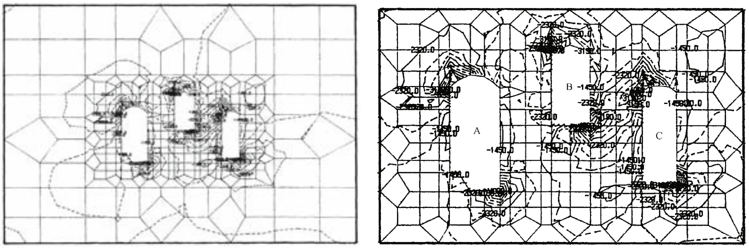

Fig. 10.21 The principal stress σ_2 around the curves

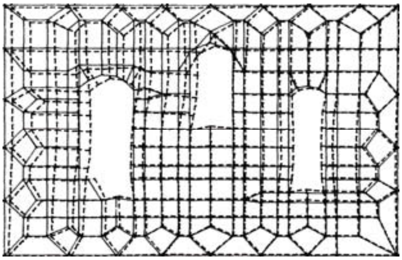

Fig. 10.22 Displacement of rock around the caves

10.5 Plastic Analysis for Underground Excavation at Laxiwa Hydraulic Power Station

10.5.1 Strength of the Laxiwa Granite

The true tri-axial experimental for the Laxiwa granite was made by the Investigation and Design Institute of Northwest China Hydroelectric Power and Wuhan Institute of Rock and Soil Mechanics of the Chinese Academy of Science (Li XC and Xu, 1994). Five groups of experiments on stress angles (θ=0°, 13.9°, 30°, 46.1°, 60°) were carried out under a hydrostatic pressure of p=130 MPa. The test results and limit locus in the π-plane for granite under hydrostatic pressure

p=130 MPa are shown in Fig. 10.23 (Li XC and Xu, 1990).

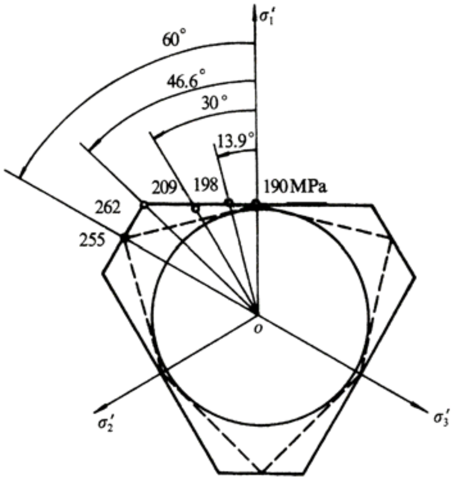

Fig. 10.23 Limit locus in the π-plane for granite (Li and Xu, 1990)

The following can be seen.

1) The length of vector q differs corresponding to different stress angles of θ in the π-plane when the hydraulic pressure p is constant. Granite shows an obvious stress angle effect. There is an obvious distinction between the circular limit loci of the Drucker-Prager criterion and the experimental results.

2) All the experimental points are located outside the limit loci of the Mohr-Coulomb strength theory and they are closer to that of the twin-shear strength theory.

3) In the process of varying the stress angle from θ=0° to θ=60°, the value of q increases and reaches q=262.2 MPa. It then decreases to q=255 MPa. This result agrees with the twin-shear strength theory.

So the twin-shear strength theory was used for the plastic analysis of underground excavation at Laxiwa Hydraulic Power Station. Other criteria are also used for comparison. The results are given to show how they are influenced by the yield criteria. The twin-shear unified strength theory was also used by Sun et al. (2004) at Zhejiang University and the East China Investigation and Design Institute, State Power Corporation of China for the Tai'an Pumped Storage Hydraulic Power Station in Shandong Province, China.

10.5.2 Plastic Zones Around the Underground Excavation Using the Single-Shear and Twin-Shear Theories

The spreads of the plastic zones under the ground stresses were obtained by using the Mohr-Coulomb strength theory (unified strength theory with *b*=0) and the twin-shear strength theory (unified strength theory with *b*=1) as shown in Fig. 10.24. It is seen that the area of the plastic zone of the twin-shear strength theory is less than the plastic zone of the Mohr-Coulomb strength theory (single-shear theory or the unified strength theory with *b*=0). According to the calculation made by the Northwest China Hydroelectric Power Investigation and Design Institute, if the area of the plastic zone around the underground excavation obeys the single-shear theory, it is 100% of the total area. Then the area of the plastic zone around the underground excavation that obeys the twin-shear theory is 44% of the total area.

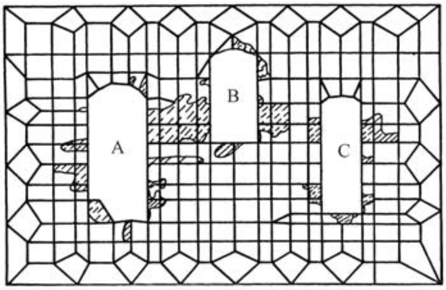

(a) UST with *b*=0 (Single-shear theory)

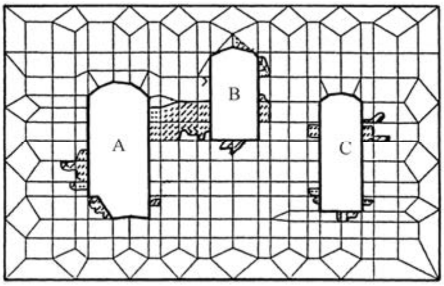

(b) UST with *b*=1 (Twin-shear theory)

Fig. 10.24 lastic zone around underground excavation

According to the convexity of the yield surface, some smooth models and two bounds are shown in Fig. 18.25, in which the limit locus 1 is the Mohr-Coulomb strength theory (1900), locus 2 is the twin-shear strength theory (Yu et al., 1985), locus 3 is the William and Warnke criterion (1975), locus 4 is the twin-shear smooth model (Yu and Liu, 1990a; 1990b) and locus 5 is the Gudehus-Argyris criterion.

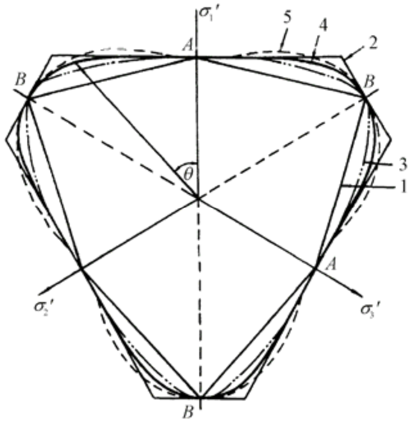

Fig. 10.25 Some smooth yield loci and two bounds of the convex yield loci

The distribution of the plastic zone around the underground excavation with the Gudehus-Argyris yield criterion is shown in Fig. 10.26.

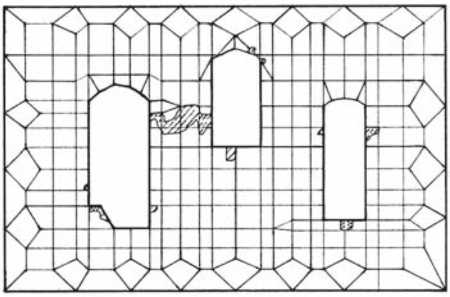

Fig. 10.26 Plastic zone around underground excavation (Gudehus-Argyris criterion)

10.5.3 Plastic Zones Around the Underground Excavation with Four Yield Cone Criteria

The yield loci of four yield cone criteria are shown in Fig. 10.27. They are (a) extended cone; (b) inscribed cone (Drucker-Prager criterion); (c) compromise cone; (d) compressive cone. The plastic zone around the underground excavation with four yield cones is shown in Fig. 10.28.

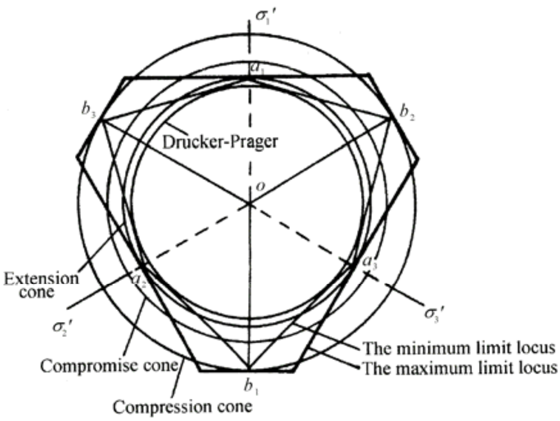

Fig. 10.27 Limit loci of various failure criteria on the deviatoric plane

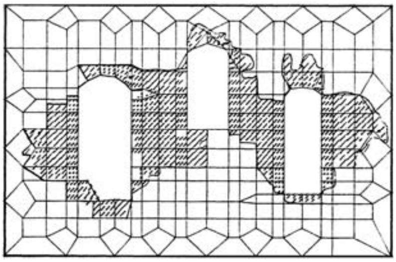

(a) Extended cone

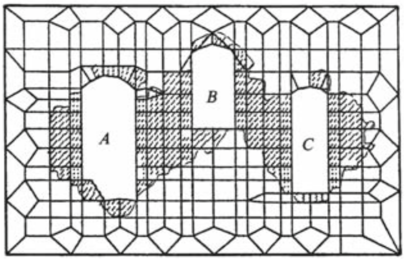

(b) Inscribed cone (Drucker-Prager criterion)

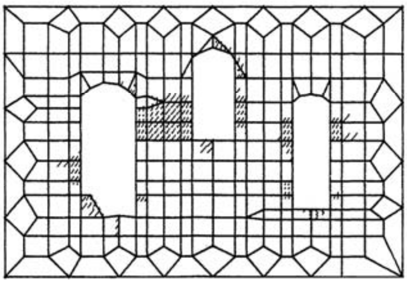

(c) Compromise cone

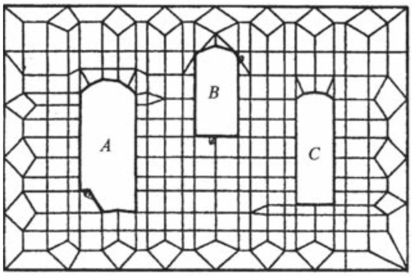

(d) Compressive cone

Fig. 10.28 Plastic zone around underground excavation with four yield cones

10.6 The Effect of Failure Criterion on the Plastic Zone of the Underground Excavation

A great deal of research has been dedicated to showing the effects of failure criteria on the analytical results of load-carrying capacities of structures. A famous example was given by Humpheson and Naylor (1975), and was further studied by Zienkiewicz and Pande (1977). They show a great difference between results obtained by using various failure criteria. Obviously, the question arises as to which one of these results should be preferred, because there is only one reasonable result for a given material and structure.

As pointed out by Zienkiewicz and Pande (1977), the choice of the best limit surface is still in the hands of the analyst who has modeled the strength behaviour in the best possible manner. They also indicated that the Drucker-Prager criterion and the limit loci of circular cones give a very poor approximation to the real failure conditions (Humpheson and Naylor, 1975; Zienkiewicz and Pande, 1977).

Most of the limit surfaces of different failure criteria are cones in the stress space. The limit loci in the meridian plane are linear. This means that the strength of materials is linearly dependent on the hydrostatic stress in the range of lower and median hydrostatic stresses, as has been demonstrated in a number of tests. The differences between the limit loci of various failure criteria in the deviatoric plane are shown in Fig. 10.25 and Fig. 10.27.

The experimental data of true triaxial tests done by the Investigation and Design Institute of Northwest China Hydroelectric Power, Ministry of the Power Industry, Ministry of Water Resources, the China Institute of Rock and Soil Mechanics, are higher than the Mohr-Coulomb single-shear theory and close to the twin-shear theory.

In this example, the twin-shear theory is applied to the plastic analysis of underground excavation at Laxiwa Hydraulic Power Station, because the experimental results for underground rock (granite) at the Laxiwa area obtained by the Investigation and Design Institute of Northwest China Hydroelectric Power and Wuhan Institute of Rock and Soil Mechanics of Chinese Academy of Science agree well with the twin-shear strength theory, as shown in Fig. 10.23 (Liu, 1994; 1995; Liu and Wu, 1995; Sun, 1998). The plastic zone around the underground excavation is shown in Fig. 10.24(b). A conclusion was made therefore by the Investigation and Design Institute of Northwest China Hydroelectric Power that "The area of the plastic zone obeying the twin-shear theory is only 0.44 times the area of the plastic zone obeying the single-shear theory. Using the twin-shear unified strength theory can reduce considerably the amount of support work and save a lot of investment. It will be a significant economic benefit. Preliminary estimates show that up to 15 million RMB Yuan can be saved."

10.7 Three Dimension Numerical Modeling of Underground Excavation for a Pumped-Storage Power Station

A pumped-storage scheme is a type of power station for storing and producing electricity to supply high peak demands by moving water between reservoirs at different elevations. In general, water is channeled from a high-level reservoir to a low-level reservoir, through turbine generators that generate electricity. This is done when the station is required to generate power. During low-demand periods, such as overnight, the generators are reversed to become pumps that move the water back up to the top reservoir.

The Tai'an Pumped Storage Hydraulic Power Station has been constructed in Shandong Province, China. The upper water reservoir of the storage power station on the top of the mountain is shown in Fig. 10.29. It has a total capacity of 1000 MkW.

Fig. 10.29 Top water reservoir of the Tai'an Pumped Storage Hydraulic Plant

3D finite element numerical modeling of the excavation rock mass of Tai'an Pumped Storage Hydraulic Power Station was done by Professors Sun, Shang, Zhang et al. of Zhejiang University, Hangzhou, China and East China Investigation and Design Institute, State Power Corporation of China (Sun et al., 2004a; 2004b).

The rock mass failure of an underground excavation often begins with local instability (failure of rock).

The initial failure position is the weak part of the surrounding rock mass. It would not take too much money to reinforce the rock mass if the weak position of the rock mass can be found and reinforced reasonably. The failure of the surrounding rock mass may be caused by the lower strength of the rock mass somewhere. Also, it may be caused by the accumulation of stress on the underground excavation. The local failure of the rock mass caused by stress accumulation during excavation can be forecast by numerical modeling analysis.

The weak position may not be located in the middle part of the excavation, but may be located at a certain distance from the end of the excavation. This has been proven by the outcome of the 3D finite element numerical modeling study of the excavated rock mass at the Tai'an Pumped Storage Hydraulic Power Station. Therefore, based on 2D numerical simulation results of the middle part of the excavation, the reinforced design may be unsafe. In order to make a reasonable evaluation of the excavation area, the weak position in the surrounding rock mass should be determined by 3D numerical modeling. In this analysis, the twin-shear unified strength theory proposed by Yu is used (Sun et al., 2004a; 2004b).

The isograms of the major principal stress and minor stress in the middle of the excavation and their variety at elastic range are shown in Figs. 10.30 to 10.32.

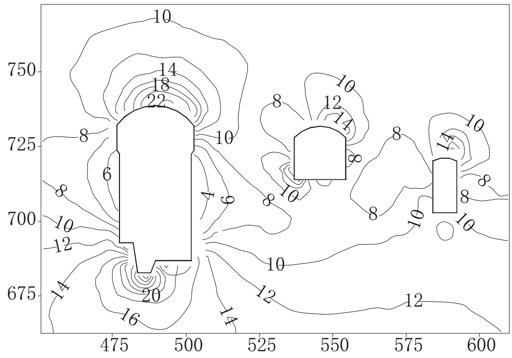

Fig. 10.30 Isograms of major principal stress

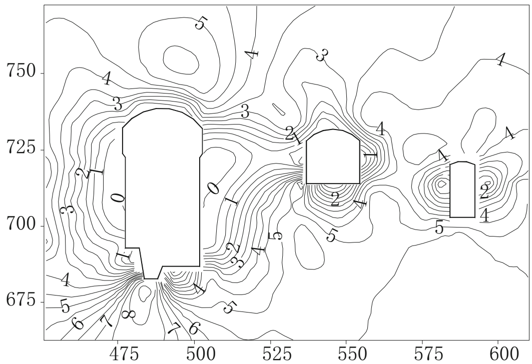

Fig. 10.31 Isograms of minor principal stress

A map of the excavation and analysed section locations is shown in Fig. 10.33. The plastic zones of the underground excavation are calculated in terms of the twin-shear unified strength theory. Three calculated results of the plastic zone of the underground excavation are obtained. The plastic zones of the underground excavation of section *A*-*A* and section *B*-*B* are shown in Figs. 10.34 and 10.35, respectively. The failure zone of surrounding rock of *C*-*C* section is rather small.

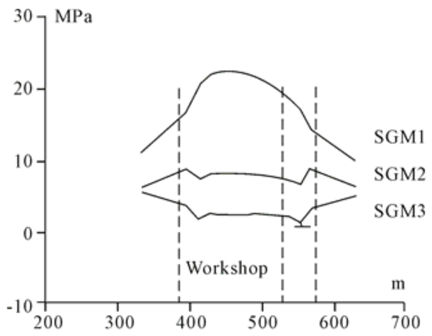

(a) At the top of cave

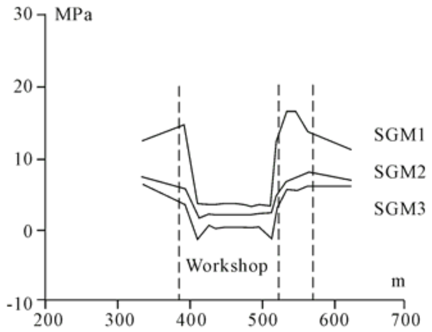

(b) At the wall of cave

Fig. 10.32 Principal stress variation along the excavation axis

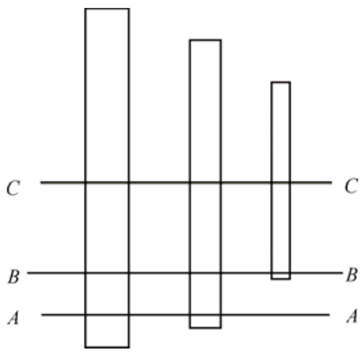

Fig. 10.33 Map of the excavation locations

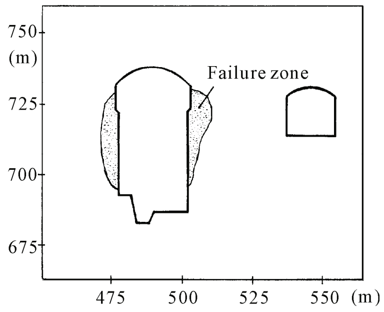

Fig. 10.34 Failure zone of surrounding rock (*A-A* section)

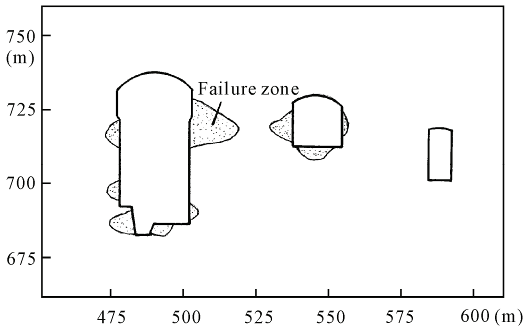

Fig. 10.35 Failure zone of surrounding rock (*B-B* section)

According to the feature of the failure zone of the surrounding rock between the caves, the failure zone of surrounding rock at section *C-C* is very small. The surrounding rock is stable. However, the section to the side of the middle position of the surrounding rock still contains several destructive areas, as shown in Fig. 10.35. Therefore, we should increase the anchor intensity and anchor rod length in these sections to guarantee the stability of the surrounding rock. Several design proposals were presented by Sun et al. (2004).

The research of Professers Sun and Shang was adopted for application at the Tai'an Pumped Storage Hydraulic Power Station. The excavation of underground caves was carried out in six parts, as shown in Fig. 10.36. Distributions of the surrounding rock rupture zone of a typical section after the fifth excavation and sixth excavation are shown in Figs. 10.36 and 10.37 (Sun et al., 2004).

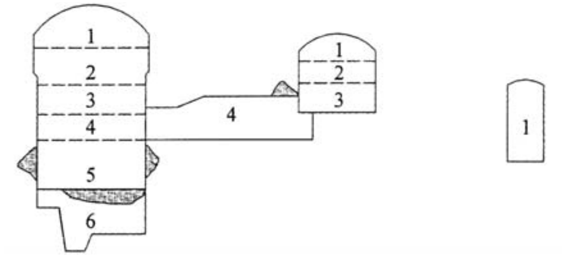

Fig. 10.36 Distribution of surrounding rock rupture zone of typical section after fifth excavation

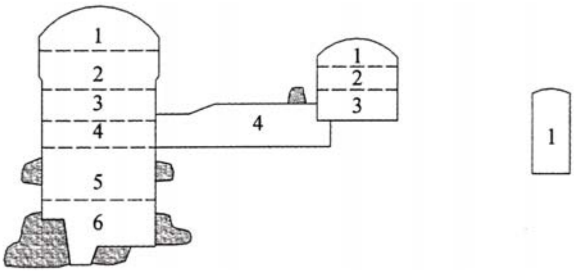

Fig. 10.37 Distribution of surrounding rock rupture zone of typical section after sixth excavation

10.8 Dynamic Response and Blast-Resistance Analysis of a Tunnel Subjected to Blast Loading

This work was done by professors Liu GH and Wang ZY at Zhejiang University, Hangzhou, China, for a railroad tunnel (Liu and Wang, 2004). The twin-shear unified strength theory is also used for dynamic problems.

In recent years, research on the structural characteristics of demolition under the load function has invited widespread interest. Ultra short distance demolition appraisal is one of the research topics in this domain.

The blast with a short distance is harmful to an existing tunnel, which is the key problem in the practical engineering. Dynamic analysis and unified strength theory were applied to develop appropriate methods for evaluating the tunnel's safety and to devise an optimal blasting scheme for nearby blasting by Prof. Liu at Zhejiang University. Blasting dynamic analysis results are used to plot the time-course curves and the frequency spectrum of the structural response. A case study is presented to illustrate the rational benefits of the above theory and method.

Displacement vector fields for a railroad tunnel, when the source of the explosion is 15 m away and explosive charges Q=32.4 kg are used, are shown in Fig. 10.38.

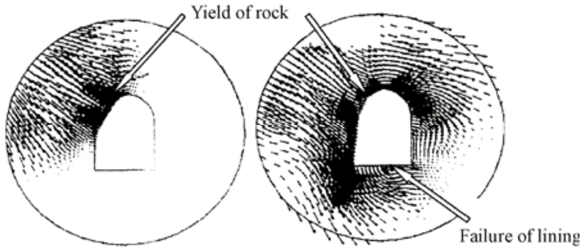

(a) Q=32.4 kg, t=5.6 ms (b) Q=32.4 kg, t=8.2 ms

Fig. 10.38 Displacement vector fields of railroad tunnel under all blasting (Q=32.4 kg)

Attenuation of vibration velocity, with the distance between explosion source and the tunnel for an existing tunnel, are shown in Fig. 10.39. If the simulated result of the explosion has a total explosive charge of Q=32.4 kg, the response is great.

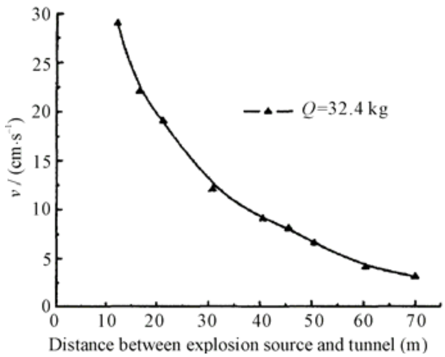

Fig. 10.39 Attenuation of vibration velocity with distance between explosion source and tunnel

When the whole explosion causes adverse vibration effects on the tunnel, the use of a step-blasting technique can effectively reduce the vibration response. Displacement vector fields for a railroad tunnel, when the explosion source is 15m away and step explosive charges of Q=6 kg are used, are shown in Fig. 10.40. The displacement vector fields for a railroad tunnel are shown in Fig. 10.41. Obviously, the dynamic response has decreased significantly. When the whole explosion (32.4 kg) is divided into 7 steps, the dynamic response of step blasting explosives (the largest step explosive amount is 6 kg) in the numerical simulation results is shown in Fig. 10.41.

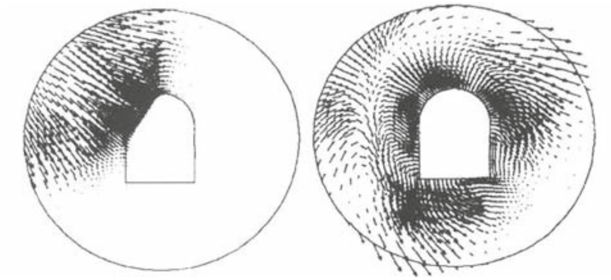

(a) Q=6 kg, t=5.6 ms (b) Q=6 kg, t=8.2 ms

Fig. 10.40 Displacement vector fields of railroad tunnel under step blasting (Q=6 kg)

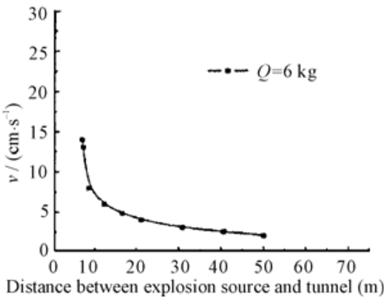

Fig. 10.41 Attenuation of vibration velocity with distance between explosion source and tunnel

Some key dynamic problems of the underground blasting structure were studied by Liu GH and Wang ZY for a railroad tunnel. The blasting safety assessment and optimal selection of construction methods are discussed in detail, in which the twin-shear strength criterion is adopted as the basic theory. The dynamic analysis method with twin-shear strength theory can not only be used for the spectrum characteristics of the dynamic response, but also for the stress analysis and security assessment of tunnel engineering.

We can study the dynamic response and blast-resistance analysis of a tunnel subjected to blast loading based on the stress state of the rock mass and failure criteria, in which the twin-shear strength theory is adopted as a failure criterion. The blasting construction plane, according to this theory and method, are adopted for use in practical railroad engineering.

10.9 Brief Summary

The numerical simulations of the effect of yield criterion on the plastic zone for an underground circular cave under vertical compression and two direction compressions, the stability of surrounding rock of the underground excavation of the Laxiwa Hydraulic Power Station on the Yellow River, 3D numerical modeling of the underground excavation for a pumped-storage power station, and the dynamic response and blast-resistance analysis of a tunnel subjected to blast loading are described above.

The numerical results show that the prediction of the numerical simulation of structural strength is influenced strongly by the choice of the yield criterion. The effect of the yield criterion on the bearing capacity and the plastic zone of underground caves in the tunneling and excavation of a hydraulic power station is obvious. It is very important to choose a reasonable strength theory (yield criteria or material model in FEM code) in the research and design.

The change in shape and size of the yield surface of various yield criteria is great. The two bounds and region of yield criteria for materials are important. The lower bound, the upper bound and the median yield loci are the three basic yield criteria for convex yield criteria.

The results of research and design are strongly dependent on the choice of strength theory in most cases. The selection of the correct strength theory becomes even more important than anything else. A better choice of strength theory will be demanded in research and engineering applications in future. When it becomes necessary to adopt a criterion for use, it is important to experimentally check the criterion, or to investigate the experimental data in the literature. If this is not done, then very exact numerical procedures or commercial codes may lead to completely worthless results. It is important therefore to facilitate the choice of a model (Zienkiewicz and Taylor, l989).

A large number of material models have been proposed throughout the years. So far, no general model that can simulate all these variations has been presented. Therefore, several models are normally implemented in commercial programs to allow for simulations of different materials under various conditions. It is obviously of great importance to choose a constitutive model suitable for the material and the problem under consideration, as well as to assign proper values to the parameters included in this model.

The unified strength theory and associated flow rule provide us with systematic yield criteria from the lower bound to upper bound, an effective approach and a powerful tool for computational plasticity. This takes into account the effect of the intermediate principal stress and the effect of the stress angle on the strength of geomaterials. The unified strength theory has a simple mathematical formula; it can not only make better use of the strength of materials than the single-shear strength theory, but is also in wide agreement with the experimental results for different materials. The material parameters of the unified strength theory are the same as the material parameters used in the Mohr-Coulomb criterion.

According to the research results provided by the Investigation and Design Institute of Northwest China Hydroelectric Power, the spreads of the plastic zones under the ground stresses were obtained using the Mohr-Coulomb strength theory (unified strength theory with b=0) and the twin-shear strength theory (unified strength theory with b=1). It is seen that the area of the plastic zone obeying the twin-shear strength theory is less than the plastic zone of the Mohr-Coulomb strength theory (single-shear theory or the unified strength theory with b=0). If the area of the plastic zone around the underground excavation that obeys the single-shear theory is 100% of the total area, then the area of the plastic zone around the underground excavation that obeys the twin-shear theory is 44% of the total. Underground excavation engineering involves a large amount of work and has a long construction period. Owing to the experimental results of the true triaxial tests for the surrounding rock (Laxiwa granite) close to the twin-shear theory, The Investigation and Design Institute of Northwest China Hydroelectric Power came to the conclusion that, according to the twin-shear theory, the design will be a significant economic benefit.

References

An M (1990) Elasto-plastic analysis for excavation of a large hydropower station. Master's thesis of Xi'an Jiaotong University, Xi'an, China (in Chinese).

An M, Yu MH and Wu X (1991) Applications of generalized twin-shear yield criterion in rock mechanics. Rock Soil Mech., 12(1): 17-26 (in Chinese, English abstract).

Brady BHG and Brown ET (1985) Rock Mechanics for Underground Mining. London: George Allen & Unwin Ltd.

Dhawan KR, Singh DN, Gupta ID (2002) 2D and 3D finite element analysis of underground openings in an inhomogeneous rock mass. Int. J. Rock Mechanics and Mining Sciences, 39(2): 217-227.

Goodman RE (1989) Introduction to Rock Mechanics. John Wiley & Sons: New York.

Hudson JA and Harrison JP (1997) Engineering Rock Mechanics: An Introduction to the Principles. Elsevier Science.

Harrison JP and Hudson JA (2000) Engineering Rock Mechanics: Illustrative Worked Examples. Elsevier Science.

Humpheson C and Naylor DJ (1975) The importance of the form of the failure criterion. C/R/243/75, University of Wales, Swansea, UK.

Jacnto AC, Ambrosnir D, and Danesir F (2001) Experimental and computational analysis of plates under air blast loading. Int. J. Impact Engineering, 25: 927-947.

Krauthammer T (1999) Blast-resistant structural concrete and steel connections. Int. J. of Impact Engineering, 22: 887-910.

Li XC, Xu DJ, Liu SH and An M (1994) The experimental research of the strength, deformation and failure properties of Laxiwa granite under the status of true triaxial stresses. Proc. Third Conf. of Chinese Society for Rock Mechanics and Engineering. China Science and Technology Press: Beijing, pp 153-159 (in Chinese, English abstract).

Liu GH and Wang ZY (2004) Dynamic response and blast-resistance analysis of a tunnel subjected to blast loading. Journal of Zhejiang University (Engineering

Science), 38(2): 204-209 (in Chinese).
Liu SH (1994) Study on the stability of surrounding rock of large underground powerhouse caverns of the Laxiwa Hydropower Project in high crustal stress area (Part One). Northwest China Water Power, (4) (Total 50): 39-43 (in Chinese).
Liu SH (1995) Study on the stability of surrounding rock of large underground powerhouse caverns of the Laxiwa Hydropower Project in high crustal stress area (Part Two). Northwest China Water Power, (1) (Total 51): 45-48 (in Chinese).
Liu SH, Wu X (1995) LAXIWA: Upland areas of large underground powerhouse and stability of surrounding rock of large underground caverns. Hydropower (WATER POWER), (3): 17-21 (in Chinese).
Pellet F, Benoit O (1999) 3-D numerical simulation of the behavior of underground structures crossing faults zone. In: Vouille G, Berest P, ed. Proc. 9th Int. Congress on Rock Mechanics. A A Balkema: Rotterdam, pp 213-218.
Sun J (1999) Rheology Theory and Its Engineering Applications. China Building Industry Press: Beijing (in Chinese).
Sun HY, Shang YQ, Zhang CS (2004a) Numerical modeling analysis for the stability of surrounding rockmass of large underground excavations. J. Zhejiang University (Engineering Science), 38(1): 70-74 (in Chinese, English abstract).
Sun HY, Shang YQ, Zhang CS, Ying HP, Li SQ (2004b) 3-D Numerical modeling of possible failure location in underground excavation. Chinese J. Rock Mechanics and Engineering, 23(123): 2192-2196 (in Chinese, English abstract).
Sun ZM (1995) Study on the dam, reservoir water and the dam foundation interaction under static and dynamic force. Northwest Hydropower, (4): 12-24 (in Chinese).
Sun ZM (1998) Dam and reservoir water, as well as dynamic and static analysis of the dam foundation interaction. Hydropower (Water Power), (3): 9-13,6 (in Chinese).
Wittke W (1990) Rock Mechanics: Theory and Applications with Case Histories. Springer-Verlag: Berlin (Germany edn. 1984)
Yan DJ, Qiang IH and Tang DG (2001) Reliability of isolation system under blast shock and vibration. China Civil Engineering Journal, 34(3):23-28 (in Chinese).
Yu MH, He LN and Song LY (1985) Twin shear stress theory and its generalization. Scientia Sinica (Sciences in China), English edn. Series A, 28(11):1174-1183.
Yu MH and He LN (1991) A new model and theory on yield and failure of materials under complex stress state. In: Mechanical Behaviour of Materials-6, Vol. 3. Pergamon Press: Oxford, pp 841-846.
Yu MH (1992a) A new system of strength theory. Xian Jiaotong University Press: Xi'an (in Chinese).
Yu MH (1998) Twin-shear Theory and Its Applications. Science Press: Beijing (in Chinese).
Yu MH (2002) Advances in strength theories for materials under complex stress state in the 20th Century. Applied Mechanics Reviews ASME, 55(3):169-218.

Yu MH (2004) Unified Strength Theory and its Applications. Springer: Berlin.
Zhang MY (1996) High arch dam: the key scientific and technological research findings. Hydropower (Water Power), 8 (in Chinese).
Zhou WY and Yang Q (2005) Numerical Computational Methods for Rock Mechanics. China Electric Power Press: Beijing.
Zienkiewicz OC (1971) The Finite Element Method in Engineering Science. McGraw-Hill: London.
Zienkiewicz OC and Pande GN (1977) Some useful forms of isotropic yield surfaces for soil and rock mechanics. Finite Elements in Geomechanics. Gudehus G ed. Wiley: London, pp 179-190.
Zienkiewicz OC and Taylor RL (l989) The Finite Element Method, vol. l, 4th edn, McGraw-Hill: London, New York.